Constraining solar hidden photons using HPGe detector

R. Horvat, D. Kekez*, M. Krčmar, Z. Krečak, A. Ljubičić

Rudjer Bošković Institute, P.O.Box 180, 10002 Zagreb, Croatia

Abstract

In this Letter we report on the results of our search for photons from a U(1) gauge factor in the hidden sector of the full theory. With our experimental setup we observe the single spectrum in a HPGe detector arising as a result of the photoelectric-like absorption of hidden photons emitted from the Sun on germanium atoms inside the detector. The main ingredient of the theory used in our analysis, a severely constrained kinetic mixing from the two U(1) gauge factors and massive hidden photons, entails both photon into hidden state oscillations and a minuscule coupling of hidden photons to visible matter, of which the latter our experimental setup has been designed to observe. On a theoretical side, full account was taken of the effects of refraction and damping of photons while propagating in Sun's interior as well as in the detector. We exclude hidden photons with kinetic couplings $\chi > (2.2 \times 10^{-13} - 3 \times 10^{-7})$ in the mass region 0.2 eV $\lesssim m_{\gamma'} \lesssim$ 30 keV. Our constraints on the mixing parameter χ in the mass region from 20 eV up to 15 keV prove even slightly better then those obtained recently by using data from the CAST experiment, albeit still somewhat weaker than those obtained from solar and HB stars lifetime arguments.

Keywords: Hidden photon, Kinetic mixing, Sun
PACS: 12.60.Cn, 14.70.Pw, 96.60.Vg

The models of SUSY-breaking most oftenly involve dynamics of a hidden sector, which uses to communicate the SUSY-breaking scale (usually larger than the weak scale) to the visible sector with aid of operators having always the appropriate loop or Planck-scale suppression. Otherwise the gauge hierarchy would be destabilized. If a U(1) gauge factor is contained in the hidden sector, a new communication mechanism [1] in the form of an operator that mixes two U(1)'s opens up, having a potential to destabilize any model for SUSY-breaking. Since this operator is a renormalizable one, it comes with no suppression by the large mass scale and therefore the mixing parameter χ must be small. The fact that both in field theory and in string theory settings an appreciable amount of χ can be generated [1], one may recognize the kinetic mixing operator as an important ingredient in these fundamental theories.

Introduction of an explicit mass term for hidden photons (thereby not upsetting the renormalizability of the theory) together with the kinetic mixing term mentioned above would lead to a model of photon oscillations (photons-hidden photons) [2] similar to the much more popular neutrino flavor oscillations. To this end, one gets rid of the kinetic mixing term by the appropriate rotation of states, introducing in such a manner a truly sterile state with respect to gauge interactions. This generates a nondiagonal mass matrix in the sector of two photons, a necessary ingredient for the oscillation phenomenon. A thorough analysis of finding appropriate propagating states in vacua as well as in a matter background has been done recently [3, 4]. Thus, the flavor (or interacting) states (one truly sterile while the other with the full gauge coupling to charged matter particles) can be expressed as a linear combination of propagating states in vacua/matter. As a consequence, a sterile propagating state would gain a tiny coupling to ordinary matter of order χ in vacua, while in matter such a coupling depends on both the real and imaginary part of the photon self-energy at finite temperature/density. This is crucial for our experimental setup (see below), since after being oscillated into a sterile state and (presumably) quick absorption of the active component in ordinary matter, it is just the sterile propagating state that leaves material background and travels unscathed towards a region where it is to be detected.

In the present Letter, we aim to observe sterile photon states (hereafter denoted as γ') in a few keV range and coming from the Sun by observing the photoelectric-like process on germanium atoms inside the HPGe detector. So far the most stringent limits on the hidden-photon mixing, in the mass region relevant for our investigation, are obtained by experiments using the Sun as a source of hidden photons [3] as well as by astrophysical arguments regarding the solar lifetime [3] and HB stars lifetime [5].

The low-energy effective Lagrangian for the two-photon

*Corresponding author.
Email address: Dalibor.Kekez@irb.hr (D. Kekez)

system with kinetic mixing reads [6]

$$\begin{aligned}\mathcal{L} &= -\frac{1}{4}F^{\mu\nu}F_{\mu\nu} - \frac{1}{4}F'^{\mu\nu}F'_{\mu\nu} - \frac{1}{2}\,\chi\,F^{\mu\nu}F'_{\mu\nu} \\ &\quad + \frac{1}{2}m_{\gamma'}^2 A'^{\mu}A'_{\mu} - eA^{\mu}J_{\mu}\ , \end{aligned} \tag{1}$$

where $F^{\mu\nu}$ and $F'^{\mu\nu}$ are the photon (A^{μ}) and hidden photon (A'^{μ}) field strengths, respectively, J^{μ} is the current of electrically charged matter while $m_{\gamma'}$ is the hidden-photon mass that could arise from a Higgs or Stückelberg mechanism [7]. For transversely polarized hidden photons of energy sufficiently above the plasma frequency $\omega_{\rm p}$ (in the solar model, 1 eV $\lesssim \omega_{\rm p} \lesssim$ 295 eV) we can write the differential flux at the Earth as [3]

$$\begin{aligned}\frac{d\Phi_{\gamma'}}{dE_{\gamma'}} &= \frac{1}{\pi^2 R_{\rm Earth}^2}\int_0^{R_\odot} dr\, r^2\, \frac{E_{\gamma'}\sqrt{E_{\gamma'}^2-\omega_{\rm p}^2}}{e^{E_{\gamma'}/(k_{\rm B}T)}-1} \\ &\quad \times \frac{\chi^2 m_{\gamma'}^4}{\left(\omega_{\rm p}^2 - m_{\gamma'}^2\right)^2 + (E_{\gamma'}\Gamma)^2}\,\Gamma\ , \end{aligned} \tag{2}$$

where $E_{\gamma'}$ is the hidden-photon energy, the plasma frequency $\omega_{\rm p} = \sqrt{4\pi\alpha N_{\rm e}/m_{\rm e}}$, $k_{\rm B}$ is the Boltzmann constant, T is the solar plasma temperature, $R_\odot$ is the solar radius, $R_{\rm Earth} \approx 1.5\times10^{13}$ cm is the average Sun–Earth distance, and Γ is the damping factor given by [3]

$$\begin{aligned}\Gamma &= \frac{16\pi^2\alpha^3}{3m_{\rm e}^2E_{\gamma'}^3}\sqrt{\frac{2\pi m_{\rm e}}{3k_{\rm B}T}}N_{\rm e}\left[1-\exp(-\frac{E_{\gamma'}}{k_{\rm B}T})\right] \\ &\quad \times\sum_{\rm i} Z_{\rm i}^2\, N_{\rm i}\,\bar{g}_{\rm ff,i} + \frac{8\pi\alpha^2}{3m_{\rm e}^2}\,N_{\rm e}\ . \end{aligned} \tag{3}$$

The first term is the bremsstrahlung contribution to the damping, where index "i" designates protons or alphas, while the second term is the Compton contribution. Here it is assumed that all hydrogen and helium are completely ionized. The thermally averaged Gaunt factors $\bar{g}_{\rm ff,i}$ are taken from [8] which presents an accurate analytic fitting formula for the nonrelativistic exact Gaunt factor. The calculation is also checked using another exact formula (with numerical integration over Maxwellian distribution) [9]. The r-dependent quantities, T, $N_{\rm e}$, $N_{\rm p}$, and N_α are calculated using BS05 Standard Solar Model [10]. Our experiment is the most sensitive to hidden photons of around 1.6 keV (see below), and since they are created mostly in Sun's inner layers (as shown in Fig. 1), Eqs. (2) and (3) (ionization neglected) can be reliably applied to calculate the expected flux of hidden photons. The contribution of different solar layers to the hidden-photons flux, depicted in Fig. 1 for $m_{\gamma'} = 100$ eV, exhibits a narrow peak at $r = 0.28\,R_\odot$ corresponding to the resonant contribution, $\omega_{\rm p}^2(r) = m_{\gamma'}^2$, in the integrand of Eq. (2). The plasmon mass is maximal at Sun's center, $\omega_{\rm p}(0) \simeq 290$ eV. For $m_{\gamma'} \gtrsim 290$ eV there is no resonant contribution in Eq. (2) (and there would have been no peak in Fig. 1 had it drawn for $m_{\gamma'} \gtrsim 290$ eV). This causes a sudden drop in sensitivity for $m_{\gamma'} \gtrsim 290$ eV what can be clearly seen in Fig. 3.

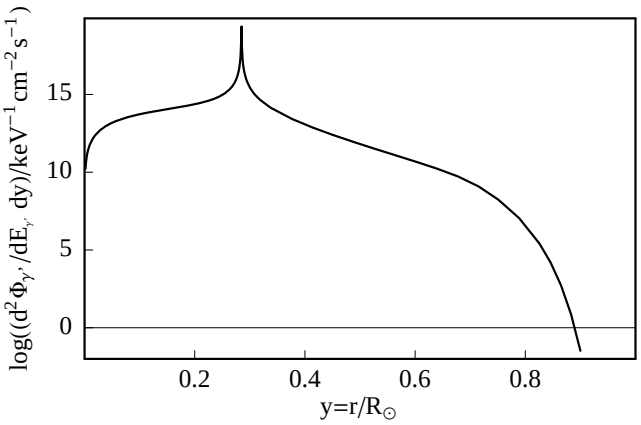

Figure 1: Flux of solar hidden photons at the Earth as a function of the normalized radial coordinate $y = r/R_\odot$ for $E_{\gamma'} = 1.6$ keV, $m_{\gamma'} = 100$ eV, and $\chi = 3\cdot10^{-13}$.

Our experiment involves searching for the particular energy spectrum in the measured data,

$$\frac{dN_{\gamma'}}{dE_{\gamma'}} = \frac{d\Phi_{\gamma'}}{dE_{\gamma'}}\sigma_{\gamma'{\rm Ge}\to{\rm Ge}^*{\rm e}}(E_{\gamma'})N_{\rm Ge}\,t\ , \tag{4}$$

produced if the hidden photons from the Sun are detected via photoelectric-like effect on germanium atoms. Here $N_{\rm Ge}$ is the number of germanium atoms in the detector and t is the data collection time. The cross section for the hidden-photon absorption, $\gamma' + {\rm Ge} \to {\rm Ge}^* + {\rm e}$, can be expressed via the cross section for the ordinary photoelectric absorption as (see, e.g., Ref. [11])

$$\sigma_{\gamma'{\rm Ge}\to{\rm Ge}^*{\rm e}}(E_{\gamma'}) = \frac{\chi_{\rm eff}^2}{\beta_{\gamma'}}\sigma_{\gamma{\rm Ge}\to{\rm Ge}^*{\rm e}}(E_{\gamma'})\ , \tag{5}$$

where

$$\chi_{\rm eff}^2 = \chi^2\left|\frac{m_{\gamma'}^2}{m_{\gamma'}^2 + 2E_{\gamma'}^2(n(E_{\gamma'})-1)}\right|^2\ , \tag{6}$$

and $\beta_{\gamma'} = \sqrt{1-m_{\gamma'}^2/E_{\gamma'}^2}$ is the velocity of the hidden photons and the data for $\sigma_{\gamma{\rm Ge}\to{\rm Ge}^*{\rm e}}$ are taken from Ref. [12]. The effective mixing parameter $\chi_{\rm eff}$ takes into account the media (germanium) influence on the photon–hidden-photon mixing. This is essentially the fraction in the second line of Eq. (2) with $\omega_{\rm p}$ and Γ expressed via the more commonly used complex refractive index n as $2E_{\gamma'}^2(1-n) = \omega_{\rm p}^2 - iE_{\gamma'}\Gamma$ (see, *e.g.*, Ref. [13]). The germanium refractive index data are taken from Ref. [14]. Because in our experimental setup the target and the detector are the same, the efficiency of the system for the expected signal is ≈1. The X-rays accompanying the photoelectric-like effect will be thereafter absorbed in the same crystal, so the energy of the particular outgoing signal equals the total energy of the incoming hidden photon.

The experimental setup used in this search for solar hidden photons has been described elsewhere [15–17]. Here

we only recall that the HPGe detector with an active target mass of 1.5 kg was placed at ground level, inside a low-radioactivity iron box with a wall thickness ranging from 16 to 23 cm. The box was lined outside with 1 cm thick lead. A low threshold on the output provided the online trigger, ensuring that all the events down to the electronic noise were recorded. Various calibrated sources have been used to study the linearity and energy resolution and, in particular, in the lowest-energy region mainly a ^{241}Am source. The detector resolution was about 820 eV for the 13.9 keV gamma-rays and 660 eV for their 3.9 keV escape peak. Data were accumulated in a 1024-channel analyzer, with an energy dispersion of 63.4 eV/channel and with data collection time of 2.38×10^7 s. In these long-term running conditions, the knowledge of the energy scale is allocated by continuously monitoring the positions and resolution of indium X-ray peaks of 24.14 keV and 27.26 keV, which are present in the measured spectra.

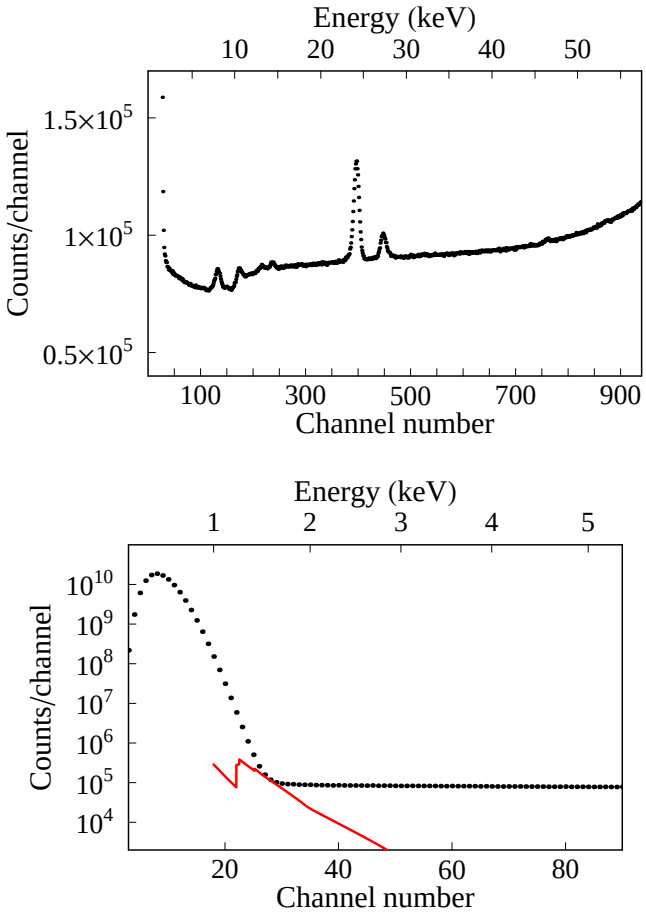

Figure 2: Top panel: total measured energy spectrum showing also X-ray peaks from various materials. Bottom panel: low-energy data shown together with the maximum of expected events due to hidden photon-electron interactions (red line), corresponding to $E_{\gamma'} \sim 1.6$ keV.

As can be seen from Fig. 2, showing the total energy spectrum, there is no evidence for any excess of photon-like events due to the hidden photon-electron interactions. The expected spectrum (red line) has a step at $E_{\gamma'} \sim 1.3$ keV, corresponding to the threshold in photoelectric cross section on germanium L electrons. There is no sign of such a step in the measured spectrum that could positively identify a hidden-photon signal. Therefore, our evaluation for upper limits on the mixing parameter follows the most conservative assumption, by requiring the predicted signal $N_{\gamma'}(k)$ in every energy bin k to be less than or equal to the recorded counts $N_{\rm exp}(k)$. Namely, $N_{\gamma'}(k) \leq N_{\rm bg}(k) + N_{\gamma'}(k) = N_{\rm exp}(k)$, where $N_{\rm bg}(k)$ is the unknown background. For every fixed $m_{\gamma'}$ we raise the parameter χ till the first touch of the predicted spectrum $N_{\gamma'}(k)$ with the measured spectrum $N_{\rm exp}(k)$ in some channel k. This value of χ is our upper limit. Similar approaches have been used elsewhere (see for instance [17–21]), where direct background measurement is not possible and the signal shape is a broad spectrum on top of an unknown background spectrum. Figure 2 (bottom panel) shows that our experiment is the most sensitive to the hidden photons of energy around 1.6 keV. For fixed $E_{\gamma'}(= 1.6$ keV) and $m_{\gamma'}$, the theoretically expected yield of hidden photon-induced events has been calculated by means of Eq. (4), where χ^4 is the only free parameter which is then used to fit the maximal strength of the expected spectrum, marked with red line in Fig. 2 (bottom panel), to the measured one. For the highest hidden-photon masses under considerations, $m_{\gamma'} \sim 10$ keV, the energy at which expected spectrum touches the measured one, shifts from fixed $E_{\gamma'} = 1.6$ keV to $E_{\gamma'} > m_{\gamma'}$. In order to estimate a day-night variation of the flux of hidden photons in our experiment (performed in Zagreb, $\varphi = 45°45^{'}$ N), which is expected due to their travel through Earth's mantle[1] ($2R_{\rm E}\cos\varphi \sim 8.9{\times}10^3$ km in length), we calculated the absorption under the most conservative assumptions that Earth's mantle consists only of iron, and its density is the mean density of the Earth. It was found that the day-night correction does not affect our limits on the mixing parameter, for the hidden-photon mass range displayed in Fig. 3.

The corresponding upper limits on the mixing parameter obtained in this work are displayed in Fig. 3 together with the current hidden photon bounds [3, 5].

In conclusion, we have performed an experiment to obtain the upper limits on the photon–hidden-photon mixing parameter χ in the eV to keV hidden-photon mass range by observing the photoelectric-like process on germanium atoms inside the HPGe detector impinged by hidden photons coming from the Sun. We have excluded hidden photons with mixing parameters $\chi > (2.2 \times 10^{-13} - 3 \times 10^{-7})$ in the mass region 0.2 eV $\lesssim m_{\gamma'} \lesssim$ 30 keV. We then compared our limits on the interaction strength χ with respect to the hidden-photon mass, to that derived recently

[1] Earth's mantle is thought to be dominantly oxygen (44.8%), silicon (21.5%), and magnesium (22.8%) with some (5.8%) iron and the remainder aluminum, calcium, sodium, and potassium.

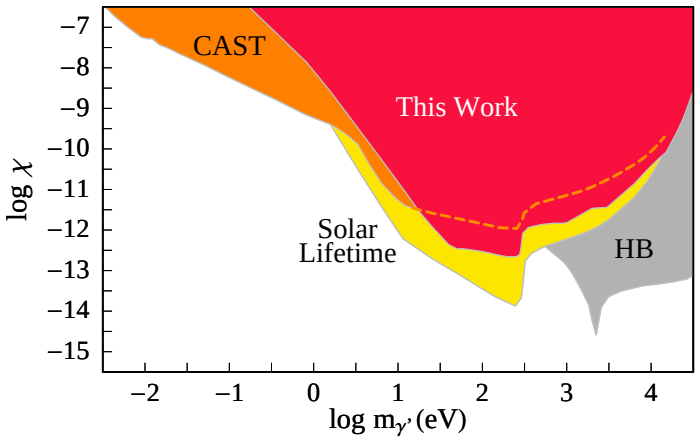

Figure 3: Limits on the mixing parameter as a function of the hidden-photon mass from this experiment against the current hidden photon bounds taken from [3, 5]. For description see the text.

[3] using helioscope data from the CAST experiment [22], as well as to those obtained from solar [3] and HB stars [5] lifetime arguments. It turns out that our limits in the hidden-photon mass region from 20 eV up to 15 keV are slightly better than those obtained from CAST laboratory measurement [3], but still somewhat weaker than those obtained from astrophysical considerations (solar and HB lifetimes). The relevance of our results lies in the fact that they constitute the best laboratory limits in the said parameter range obtained to date.

We would like to thank J. Redondo for useful comments. The authors acknowledge the support of the Croatian MSES Project No. 098-0982887-2872.

References

[1] K. R. Dienes, C. F. Kolda, J. March-Russell, Kinetic mixing and the supersymmetric gauge hierarchy, Nucl. Phys. B 492 (1997) 104–118. arXiv:hep-ph/9610479, doi:10.1016/S0550-3213(97)00173-9.

[2] H. Georgi, P. Ginsparg, S. L. Glashow, Photon oscillations and cosmic background radiation, Nature 306 (1983) 765–766. doi:10.1038/306765a0.

[3] J. Redondo, Helioscope Bounds on Hidden Sector Photons, JCAP 0807 (2008) 008. arXiv:0801.1527, doi:10.1088/1475-7516/2008/07/008.

[4] J. Redondo, M. Postma, Massive hidden photons as lukewarm dark matter, JCAP 0902 (2009) 005. arXiv:0811.0326, doi:10.1088/1475-7516/2009/02/005.

[5] J. Jaeckel, A. Ringwald, The Low-Energy Frontier of Particle Physics, Ann.Rev.Nucl.Part.Sci. 60 (2010) 405–437. arXiv:1002.0329, doi:10.1146/annurev.nucl.012809.104433.

[6] B. Holdom, Two U(1)'s and Epsilon Charge Shifts, Phys. Lett. B 166 (1986) 196. doi:10.1016/0370-2693(86)91377-8.

[7] E. C. G. Stueckelberg, Interaction energy in electrodynamics and in the field theory of nuclear forces, Helv. Phys. Acta 11 (1938) 225–244.

[8] N. Itoh, T. Sakamoto, S. Kusano, S. Nozawa, Y. Kohyama, Relativistic thermal bremsstrahlung gaunt factor for the intracluster plasma. 2. Analytic fitting formulae, Astrophys. J. Suppl. 128 (2000) 125–138. arXiv:astro-ph/9906342, doi:10.1086/313375.

[9] P. J. Brussaard, H. C. van de Hulst, Approximation Formulas for Nonrelativistic Bremsstrahlung and Average Gaunt Factors for a Maxwellian Electron Gas, Rev. Mod. Phys. 34 (1962) 507–520. doi:10.1103/RevModPhys.34.507.

[10] J. N. Bahcall, A. M. Serenelli, S. Basu, New solar opacities, abundances, helioseismology, and neutrino fluxes, Astrophys. J. 621 (2005) L85–L88. arXiv:astro-ph/0412440, doi:10.1086/428929.

[11] M. Pospelov, A. Ritz, M. B. Voloshin, Bosonic super-WIMPs as keV-scale dark matter, Phys. Rev. D 78 (2008) 115012. arXiv:0807.3279, doi:10.1103/PhysRevD.78.115012.

[12] M. J. Berger, J. H. Hubbell, S. M. Seltzer, J. Chang, J. S. Coursey, R. Sukumar, D. S. Zucker, K. OlsenXCOM: Photon Cross Section Database (version 1.5). [Online] Available: http://physics.nist.gov/xcom. National Institute of Standards and Technology, Gaithersburg, MD.

[13] J. Redondo, A. Ringwald, Light shining through walls, Contemp.Phys. 52 (2011) 211–236. arXiv:1011.3741, doi:10.1080/00107514.2011.563516.

[14] B. Henke, E. Gullikson, J. Davis, X-Ray Interactions: Photoabsorption, Scattering, Transmission, and Reflection at $E = 50 - 30,000$ eV, $Z = 1 - 92$, Atomic Data and Nuclear Data Tables 54 (2) (1993) 181 – 342, [Online] Available: http://henke.lbl.gov/optical_constants/. doi:10.1006/adnd.1993.1013.

[15] R. Horvat, D. Kekez, Z. Krečak, A. Ljubičić, Constraining theories of low-scale quantum gravity by non-observation of the bulk vector boson signal from the Sun, Phys. Rev. D 78 (2008) 127101. arXiv:0804.1659, doi:10.1103/PhysRevD.78.127101.

[16] D. Kekez, A. Ljubičić, Z. Krečak, M. Krčmar, Search for solar hadronic axions produced by a bremsstrahlung-like process, Phys. Lett. B 671 (2009) 345–348. arXiv:0807.3482, doi:10.1016/j.physletb.2008.12.033.

[17] R. Horvat, D. Kekez, M. Krčmar, Z. Krečak, A. Ljubičić, Hunting up low-mass bosons from the Sun using HPGe detector, Phys. Lett. B 699 (2011) 21–24. arXiv:1101.5523, doi:10.1016/j.physletb.2011.03.045.

[18] L. Baudis, et al., New limits on dark-matter WIMPs from the Heidelberg-Moscow experiment, Phys. Rev. D59 (1999) 022001. arXiv:hep-ex/9811045, doi:10.1103/PhysRevD.59.022001.

[19] A. Morales, C. Aalseth, F. Avignone, R. Brodzinski, S. Cebrian, et al., Improved constraints on WIMPs from the international Germanium experiment IGEX, Phys.Lett. B532 (2002) 8–14. arXiv:hep-ex/0110061, doi:10.1016/S0370-2693(02)01545-9.

[20] G. Angloher, S. Cooper, R. Keeling, H. Kraus, J. Marchese, et al., Limits on WIMP dark matter using sapphire cryogenic detectors, Astropart.Phys. 18 (2002) 43–55. doi:10.1016/S0927-6505(02)00111-1.

[21] J. Angle, et al., First Results from the XENON10 Dark Matter Experiment at the Gran Sasso National Laboratory, Phys.Rev.Lett. 100 (2008) 021303. arXiv:0706.0039, doi:10.1103/PhysRevLett.100.021303.

[22] M. Arik, et al., CAST search for sub-eV mass solar axions with ^{3}He buffer gas, Phys. Rev. Lett. 107 (2011) 261302. arXiv:1106.3919, doi:10.1103/PhysRevLett.107.261302.